

Available online at website: https://journal.bcrec.id/index.php/bcrec

Bulletin of Chemical Reaction Engineering & Catalysis, 20 (1) 2025, 112-128



Research Article

Areca catechu Biochar and Nano-Biochar as Adsorbents for Congo Red: Synthesis, Characterization, and Performance Evaluation

Robiatul Adawiyah¹, Nova Yuliasari², Yulizah Hanifah³, Neza Rahayu Palapa^{2*}

¹Master of Materials Science, Graduate Program, Sriwijaya University, Palembang, 30139, Indonesia. ²Department of Chemistry, Faculty of Mathematics and Natural Sciences, Sriwijaya University, Palembang, 30662, Indonesia

³National Research and Innovation Agency (BRIN), PUSPIPTEK, Tangerang Selatan, 15311, Indonesia.

Received: 24th December 2024; Revised: 7th February 2025; Accepted: 10th February 2025 Available online: 13th February 2025; Published regularly: April 2025



Abstract

The presence of hazardous synthetic dyes such as Congo Red in industrial wastewater poses a significant environmental threat. This study explores the potential of biochar (BC) and nano-biochar (nano-BC), derived from $Areca\ catechu$ husk as sustainable adsorbents for dye removal. Nano-BC was synthesised via hydrothermal carbonisation and mechanical ball milling, leading to enhanced structural and surface properties. X-ray Diffraction (XRD) revealed that the Pinang husk is predominantly amorphous, while BC exhibits increased crystallinity with sharp peaks, and nano-BC demonstrates the highest crystallinity and nanostructural refinement. Fourier Transform Infra Red (FTIR) confirmed the transformation of aliphatic-rich raw biomass into aromatic-dominant structures in BC and nano-BC, with nano-BC showing more pronounced graphite-like features. Scanning Electron Microscope (SEM) illustrated the morphological evolution, with nano-BC exhibiting refined, uniformly porous structures. BET analysis revealed that nano-BC has a significantly higher surface area 41.38 m²/g and smaller pore size 8.4928 nm compared to BC 22.38 m²/g and 15.39 nm, enhancing adsorption capacity. Furthermore, the adsorption kinetics followed the pseudo-second-order model, and isothermal analysis confirmed monolayer adsorption with the highest maximum adsorption capacity ($Q_{\text{max}} = 154.526 \text{ mg/g}$). These findings highlight the superior adsorption performance of nano-BC, emphasising its potential for environmentally friendly water treatment applications.

Copyright © 2025 by Authors, Published by BCREC Publishing Group. This is an open access article under the CC BY-SA License (https://creativecommons.org/licenses/by-sa/4.0).

Keywords: Nano-biochar; Congo Red; adsorption; Pinang husk; water treatment

How to Cite: Adawiyah, R., Yuliasari, N., Hanifah, Y., Palapa, N. R. (2025). Areca Catechu Biochar and Nano-Biochar as Adsorbents for Congo Red: Synthesis, Characterization, and Performance Evaluation. Bulletin of Chemical Reaction Engineering & Catalysis, 20 (1), 112-128. (doi: 10.9767/bcrec.20322)

Permalink/DOI: https://doi.org/10.9767/bcrec.20322

1. Introduction

Industrial wastewater management presents a meaningful ecological and public health threat, drastically exacerbated by the wide-ranging industrial application of synthetic dyes in diverse sectors including textiles, plastics, paper and large amounts of wastewater. This wastewater is heavily contaminated with dye and often released without proper treatment into sensitive natural water bodies [2]. The persistence of synthetic dyes, such as Congo Red, as ecological pollutants results from their important stability, large toxicity and large resistance to biodegradation [3]. Because they stay in water systems for long periods, they can disrupt many natural processes

in the water, stop some plants from making food

leather production [1]. These industries release

* Corresponding Author.

Email: nezarahayu@mipa.unsri.ac.id (N.R. Palapa)

through photosynthesis and cause serious health problems in people and animals because they can cause cancer and change genes [4]. The development of effective and sustainable wastewater treatment technologies is therefore of important importance.

Congo Red, a specific anionic diazo dye, enjoys wide-ranging use in several textile and pigment industries because of its bright color and large stability under many conditions [5]. These helpful industrial properties, however, also cause the substance to persist in the environment because standard wastewater treatment methods, such as aerobic and anaerobic digestion, are often ineffective at breaking it down [6]. The breakdown of Congo Red can create important quantities of benzidine, a carcinogen that poses a severe risk to both the environment and people [7]. Congo Red resists light, heat and oxidizing agents. This makes it very difficult to remove from wastewater [8]. Because of these important characteristics, we need to explore several new, effective and sustainable remediation strategies.

Adsorption is a greatly effective and inexpensive approach for dye removal and it stands out among many wastewater cleanup methods [9]. Despite the encouraging adsorption capacity of biochar, its performance can be significantly enhanced through reduction of the particle size to the nanoscale [10]. Nano-biochar, produced through techniques such as mechanical ball milling, exhibits a higher surface area, improved surface reactivity, enhanced dispersibility in aqueous media, and increased adsorption efficiency due to greater exposure of active adsorption sites [11]. Furthermore, nanobiochar has demonstrated superior adsorption kinetics compared to bulk biochar, allowing for more rapid and effective removal of pollutants [12]. Recent studies suggest that nano-biochar possesses enhanced electrostatic interactions, π – π interactions, and hydrogen bonding capabilities, all of which contribute to its superior adsorption performance [13]. However, limited studies have systematically explored the effect of particle size reduction on adsorption efficiency, particularly in relation to dye removal from wastewater [14].

Areca catechu (betel nut husk), a widely available agricultural byproduct, represents a promising precursor material for biochar and nano-biochar production [15].Its lignocellulosic content, structural integrity, and widespread availability in tropical regions make it an economically viable and environmentally sustainable option for adsorbent development [16]. Utilizing Areca catechu husks for nanobiochar synthesis aligns with the principles of a circular economy by promoting agricultural waste valorization and reducing environmental impact [17]. However, to date, the potential of Areca catechu-derived nano-biochar for dye removal has only been explored in a limited number of studies, and the influence of particle size reduction through high-energy milling on adsorption performance remains largely unexamined [18].

Previous studies have demonstrated the adsorption capabilities of biochar derived from various biomass sources, including orange peels [8], algae [3], waste pine needles [19], and breadfruit leaves [20], with varying levels of effectiveness in dye removal. However, there remains a critical gap in understanding the specific advantages of nano-biochar, particularly from Areca catechu husks, in enhancing adsorption efficiency [21]. Moreover, limited research has examined the influence of key process parameters, such as pH, contact time, and adsorbent dosage, on the adsorption behavior of nano-biochar [22]. Additionally, most existing studies have been conducted using synthetic dye solutions, whereas real industrial wastewater often contains complex mixtures of contaminants that may influence adsorption performance.

This study aims to address these research gaps by synthesizing and characterizing biochar and nano-biochar from Areca catechu husks for Congo Red dye adsorption. The novelty of this research lies in its systematic evaluation of the impact of nano-biochar's reduced particle size on adsorption efficiency, providing a comprehensive physicochemical characterization of adsorbents and assessing their adsorption performance in terms of capacity, kinetics, and isotherms. Additionally, this study compares the adsorption capacity of nano-biochar with other reported adsorbents and explores its adsorption mechanisms to assess its potential for large-scale application in wastewater treatment. Furthermore, the influence of critical operational parameters, such as pH, temperature, and competing ions, will be investigated to enhance the understanding of the adsorption process under realistic environmental conditions. By addressing these aspects, this research contributes to the advancement of nano-biochar applications in dye removal and highlights its potential sustainable wastewater treatment.

2. Materials and Method

2.1 Chemicals and Analyses

The materials employed in this research were distilled water ($\rm H_2O$), obtained from PT. Dira Sonita, and sodium hydroxide (NaOH) (molecular weight 40.00 g/mol, supplied by Merck), as well as hydrochloric acid (HCl) (molecular weight The materials utilized in this research included 36.458 g/mol, a 37% solution from Merck), Congo red dye ($\rm C_{32}H_{22}N_6Na_2O_6S_2$), and *Areca catechu L.*, which was collected from Pangandaran, West Java, Indonesia.

The equipments employed in this study include a Rigaku Miniflex-6000 for X-ray diffractometer analysis, Shimadzu Prestige-21 for Fourier transform infrared (FTIR) analysis, BELSORP-miniX for BET surface area analysis, the SU 8000 series for SEM morphology analysis, and an UV-Vis spectrophotometer (EMC-18PC-UV) to determine the absorbance from the filtrat.

2.2 Areca catechu Biochar Preparation

The Areca catechu husk was subjected to a cleansing process involving the removal of contaminants through the application of water. This was followed by a drying phase, conducted under solar conditions, spanning a period of 3-4 days, with the objective of reducing the moisture content. Subsequently, the material was subjected to a 12-hour heating process at 80 °C in an oven, with the objective of eliminating any residual moisture and volatile compounds. Subsequently, the husk was pulverised into a fine powder. Subsequently, the powdered particles were placed in a muffle furnace at 500 °C with a constant nitrogen gas flow of 1×103 m3/h for a period of three hours. The resulting biochar subsequently washed and then dried in a hot-air oven at 90 °C for 12 hours [19]. The characterisation of the biochar was conducted using X-ray diffraction, Fourier transform infrared spectroscopy, Brunauer-Emmett-Teller analysis and scanning electron microscopy.

2.4 Areca catechu Nano-Biochar Preparation

Nano-biochar was produced through grinding process utilising high-energy milling (HEM) at a speed of 500 rpm for a period of three hours [15]. The nano-biochar obtained from the Areca catechu fruit husk was subjected to comprehensive characterisation using advanced analytical techniques. The characterisation of the nano-biochar was conducted using a range of advanced analytical techniques, including X-ray diffraction (XRD) for the analysis of the crystalline structure, Fourier transform infrared spectroscopy (FT-IR) for the identification of functional groups on the surface, Brunauer-Emmett-Teller (BET) analysis for the evaluation of the specific surface area and pore size distribution, and scanning electron microscopy (SEM) for the investigation of the surface morphology and microstructural properties [21].

2.5 Adsorption Study

Adsorption selectivity carryout with dye solutions (Congo Red, Methyl Orange, Malachite Green, and Methylene Blue) with absorbance values measured at 0.5 nm were prepared by mixing 10 mL of each dye solution in a beaker. A

total of 0.2 g of biochar or nano-biochar was added to the anionic dye mixture and stirred for 80 minutes to ensure thorough interaction between the adsorbent and dyes. Wavelength measurements were conducted using a UV-visible spectrophotometer to monitor adsorption efficiency [26].

Various parameters, including concentration, pH, and temperature, were varied to determine the optimal conditions for the dye adsorption process. In the pH variation experiment, a 20 mL dye solution with a concentration of 15 mg/L was prepared, and its pH was adjusted within a range of 2 to 11 using NaOH and HCl solutions. After pH adjustment, the initial absorbance was measured using a UV–Vis spectrophotometer to evaluate the effect of pH on adsorption performance [27].

The adsorption experiments were conducted using 0.02 grams of biochar and nano-biochar derived from Areca catechu. The aforementioned adsorbents were placed in a 100-milliliter Erlenmeyer flask containing 20 milliliters of a Congo red dye solution with an initial concentration of 50 milligrams per liter. Prior to the commencement of the experiment, the pH of the solution was not adjusted. The mixture was agitated using a magnetic stirrer at specified time intervals of 10, 20, 30, 40, 50, 60, 90, 120, 150, and 180 minutes. Subsequently, the adsorbent was removed from the residual dye through filtration, and the resulting filtrate was collected for further analysis. The absorbance of the filtrate was determined using a UV-Vis spectrophotometer [22].

In order to investigate the thermodynamic adsorption, variations in on concentration and temperature were applied. In each experiment, 0.02 g of Areca catechu, biochar, or nano-biochar was added to 20 mL of dye solution and stirred for 90 minutes with a magnetic stirrer. The adsorption tests were conducted at four distinct temperatures. The temperatures used were 30 °C, 40 °C, 50 °C, and 60 °C. Upon completion of the stirring process, the mixtures were filtered, and the absorbance of the filtrates was measured using a UV-Vis spectrophotometer to evaluate the remaining dye concentration [23].

2.6 Adsorbent Reusability

The regeneration process was initiated by introducing the desorbed adsorbent into a 20 mL solution containing 50 mg/L of dye. The mixture was then stirred for a period of two hours, after which the remaining concentration of dye was analysed using a UV-Vis spectrophotometer. Subsequently, the adsorbent was subjected to desorption using an ultrasonic device. This entailed the mixing of 25 mL of aqueous solvent with the adsorbent, which was then stirred for a

period of two hours. The filtrate was subsequently analysed using a UV-Vis spectrophotometer. The residual material was then dried and reused in the next regeneration cycle. The quantity of the dye adsorbed (mg/g) and Q_r is the adsorption capacity of the dye after regeneration (mg/g) [24].

3. Result and Discussion

3.1. Characterizations

The X-ray diffraction (XRD) patterns of the adsorbents, namely Pinang husk, biochar (BC), and nano-BC on Figure 1, reveal distinct structural differences that are pivotal to comprehending their adsorption performance. The broad peaks observed at 2θ angles of approximately 15.66°, 22.1°, and 34.51° indicate that the pinang husk is predominantly amorphous in nature. The weak crystallinity of the pinang husk, as evidenced by the aforementioned peaks, can be attributed to its inherent organic composition and limited structural order [25].

In contrast, BC displays sharper peaks at 21.81°, 26.58°, and 35.864°, indicative of an augmented crystallinity in comparison to the unprocessed Pinang husk. These peaks are indicative of phases that are formed during the pyrolysis process, whereby organic matter decomposes, leaving behind a carbon-rich structure with enhanced order. It is noteworthy that BC also exhibits additional peaks at higher angles, such as 59.868°, which suggest the development of microcrystalline domains [26].

Nano-BC exhibits the most distinct and sharp peaks among the three adsorbents, with significant reflections at 20.870°, 25.536°, 26.628°, 35.123°, and 43.346°. The enhanced peak intensities are indicative of the improved crystallinity and structural order that has been achieved through the nanomodification process. These characteristics result in an increased surface area and a greater number of active

adsorption sites, which directly contribute to the superior adsorption performance observed [27].

The peaks observed for all adsorbents at specific angles correlate with crystalline phases, including potential indications of silica and carbon-based compounds. The more acute peaks observed in BC and Nano-BC indicate the presence of more sophisticated microstructures, which are postulated to enhance their adsorptive properties. Furthermore, the absence of specific peaks in the Pinang husk indicates that it is a raw and less processed material, which is consistent with its relatively lower adsorption capacity.

The FTIR spectra of the samples (*Areca* husk, BC, and nano-BC) on Figure 2. demonstrate substantial structural alterations resulting from thermal processing. The broad O–H stretching band at 3700–3000 cm⁻¹, which is associated with phenolic hydroxyl groups and adsorbed water, displays a reduction in intensity as the processing temperature increases. This indicates a loss of oxygen-containing functional groups. Similarly, the C–H stretching vibrations at 2924 cm⁻¹ and 2850 cm⁻¹, representing aliphatic compounds derived from cellulose and lignin, are markedly diminished in BC and Nano-BC, indicating the fragmentation of aliphatic structures into more stable aromatic forms [28].

The carbonyl (C=O) stretching vibration at 1710 cm⁻¹, present in the raw biomass, diminishes in BC and Nano-BC, indicating a conversion of ketones and esters into condensed aromatic structures. Conversely, the C=C stretching vibration at 1595 cm⁻¹, which is typical of aromatic compounds and lignin, becomes more prominent, thereby signifying increased aromaticity and the formation of polyaromatic structures [35]. Furthermore, the C–O–C stretching band at 1110 cm⁻¹, indicative of carbonyl derivatives, becomes more pronounced in Nano-BC, which is indicative of structural refinement. The peak at 770 cm⁻¹, representing aromatic C–H deformation, becomes

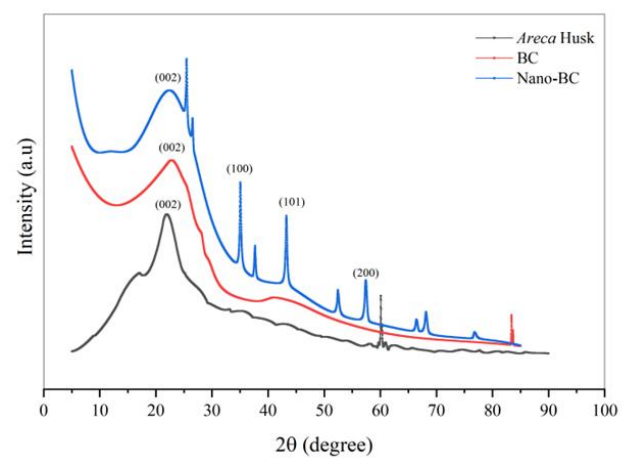


Figure 1. X-ray diffraction patern of pinang husk, biochar and nano-biochar

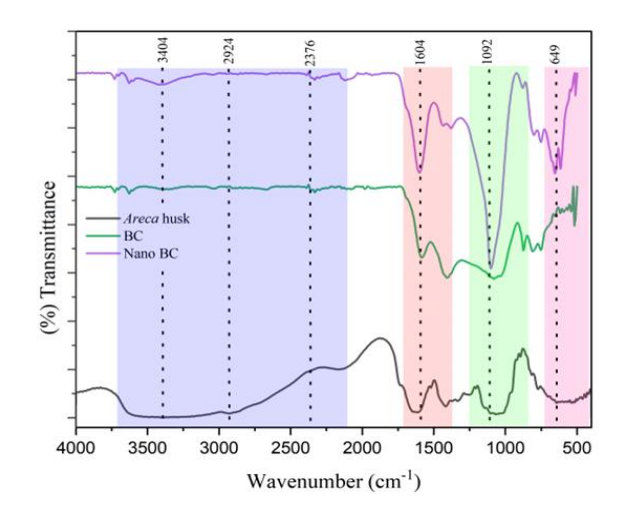


Figure 2. FTIR spectrum of areca husk, biochar and nano-biochar

more distinct in BC and Nano-BC, reflecting the development of graphite-like aromatic structures at higher temperatures [30]. Overall, these spectral changes illustrate the transformation from aliphatic-rich raw biomass to aromatic-dominant BC and Nano-BC, with Nano-BC showing the most advanced structural properties. These changes correlate with enhanced adsorption capabilities, making Nano-BC a promising material for dye removal applications.

The raw *Areca* husk (Figure 3a) has a fibrous structure with naturally occurring pores, which is essential for subsequent adsorption applications. The mean particle diameter was determined to be 5340.03 nm, indicating that the material retains a relatively coarse structure prior to pyrolysis. The presence of ridges and honeycomb pores highlights the biological origin of the husk and its potential as a precursor for biochar production.

After pyrolysis, the biochar (Figure 3b) exhibits a more porous and fragmented morphology, attributed to the release of volatile compounds during thermal decomposition. The average particle size increased significantly to 22655.40 nm, approximately 4.24 times larger than the raw husk. This increase may be related to structural changes, including the formation of a more interconnected pore network, which increases the surface area and adsorption capacity of the material [24].

Further refinement by high-energy milling resulted in nano-biochar (Figure 3c), with the particle size drastically reduced to 428.68 nm, confirming the successful conversion to the nanoscale [14]. Compared to the original *Areca* husk, the particle size reduction factor is approximately 12.46 times, and compared to biochar, it is 52.87 times smaller. The nano-

biochar has a finer particle distribution with increased surface roughness, resulting in more active sites for adsorption [37]. The transition to the nanoscale significantly improves dispersibility in aqueous media, adsorption kinetics and electrostatic interactions with anionic pollutants such as Congo Red. This transformation underlines the advantage of nano-biochar in environmental remediation, as the increased surface area of nano-biochar increases the adsorption capacity.

In this study, a BET analysis was conducted to evaluate the specific surface area and pore characteristics of biochar and nano-biochar, as presented in the table. The BET analysis revealed that the surface area of biochar is 22.38 m²/g, with an average pore size of 15.39 nm and a pore volume of 0.1301 cm³/g. In comparison, nano-biochar exhibits a markedly elevated surface area of 41.38 m²/g, accompanied by a diminished average pore size of 8.4928 nm and an augmented pore volume of 0.2095 cm³/g.

Figure 4. show that both materials display Type IV(a) physisorption isotherms, indicative of their status as mesoporous materials with pore sizes spanning the range of 2–50 nm. Furthermore, the presence of a hysteresis loop in the isotherm serves to confirm the occurrence of capillary condensation within the mesopores [34]. The adsorption process in Type IV(a) isotherms typically commences with a rapid increase in adsorption volume at low relative pressures, driven by the interaction of adsorbate molecules with higher-energy sites. This is followed by interaction with lower-energy sites as multilayer adsorption occurs [35].

The observed increase in surface area for nano-biochar in comparison to biochar can be

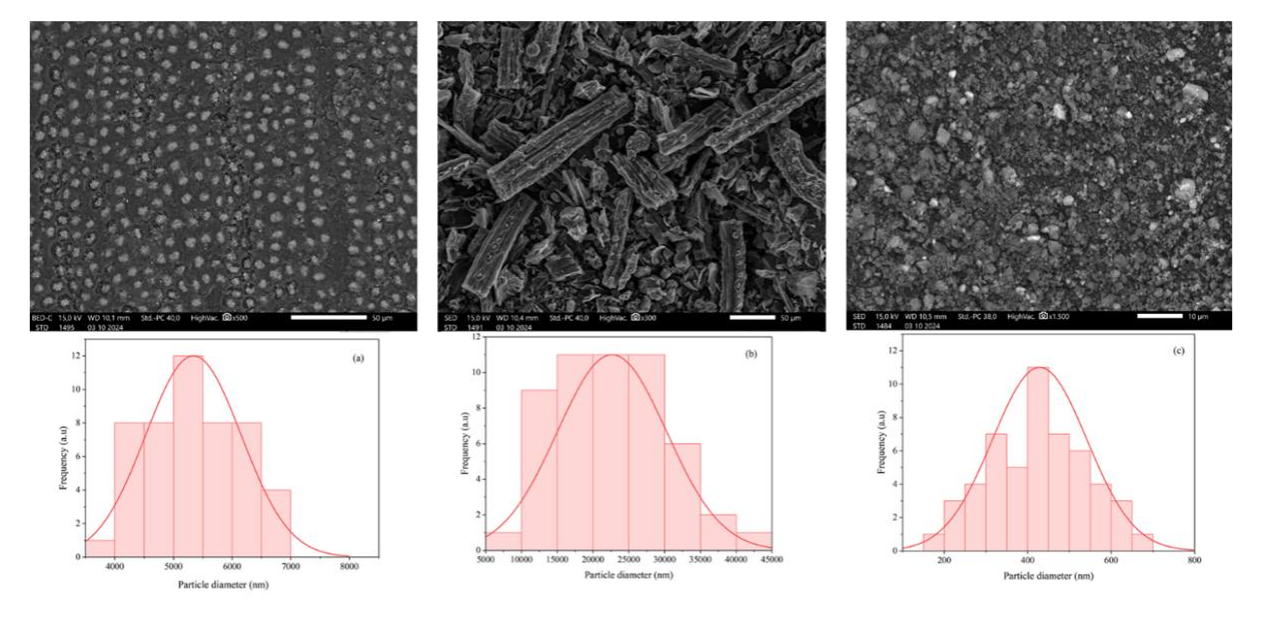


Figure 3. Scanning electron microscopy (SEM) image and particle size distribution of Areca husk (a), Biochar (b) and Nano-biochar (c).

attributed to the reduction in particle size during the nanostructuring process, which enhances the availability of active sites for adsorption [36]. The smaller pore size of nano-biochar also contributes to its higher adsorption capacity, as it facilitates stronger interactions with $_{
m the}$ molecules. The larger pore volume observed for nano-biochar indicates an increased capacity to accommodate adsorbate molecules, providing further evidence to support its superior adsorption performance [37].The results demonstrate the considerable influence of the nanostructuring process on the enhancement of specific surface area and adsorption characteristics of biochar, rendering nano-biochar a more efficacious material for applications such as dye adsorption or environmental remediation.

3.2 Dye Sorption Selectivity

Figure 5 shows. the ability of an adsorbent to selectively capture and separate specific dyes from a mixture is referred to as dye selectivity. Developing an adsorbent with high selectivity is crucial for wastewater treatment applications, as industrial effluents often contain complex mixtures of dyes and other contaminants. Enhancing the selectivity of biochar and nanobiochar towards particular dyes improves treatment efficiency, reduces chemical and energy

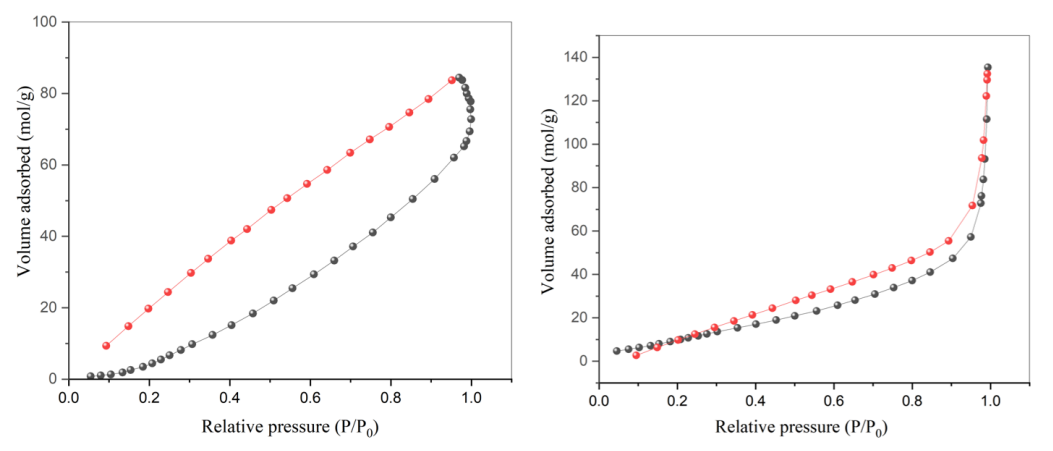


Figure 4. The N₂ adsorption/desorption isotherm of Biochar (a) and Nano-biochar (b)

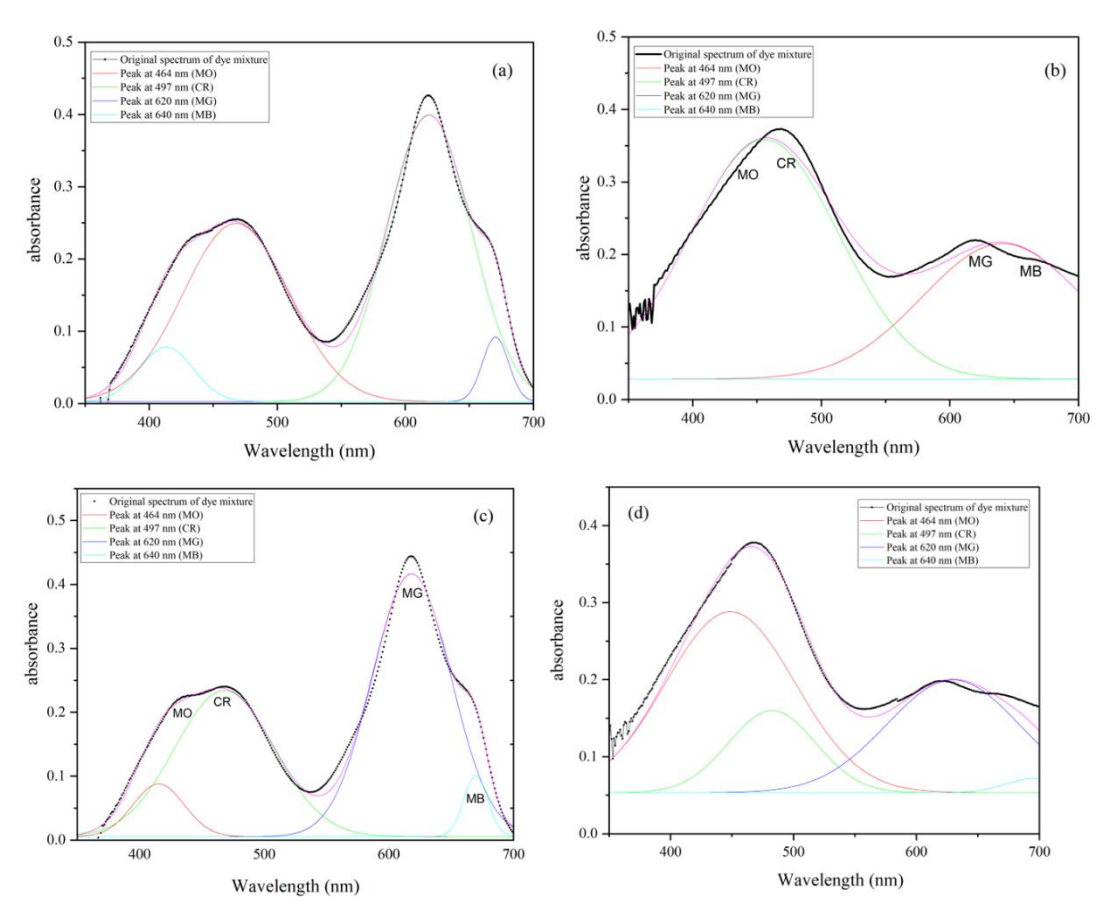


Figure 5. Deconvolution of absorbance spectra of anionic dye selectivity gaussian curve fit by adsorbent before adsorption (a,c) after adsorption by biochar (c) nano-biochar (d)

consumption, and leads to higher-quality treated water [42].

In this study, the adsorption performance of biochar and nano-biochar derived from Areca catechu husks was evaluated for Congo Red (CR), Methyl Orange (MO), Malachite Green (MG), and Methylene Blue (MB). The adsorption capacity varied among the dyes, with the highest adsorption observed for Malachite Green (60.84%) and the lowest for Methyl Orange (6.87%). Biochar exhibited lower adsorption efficiency than nano-biochar due to its larger particle size and lower surface reactivity. The enhanced adsorption capability of nano-biochar can be attributed to its increased surface area, higher porosity, and greater availability of active functional groups [43].

Spectral deconvolution of the UV-Vis absorption spectra before and after adsorption was conducted to assess dye selectivity, as shown in Figure 6. Due to overlapping absorption peaks in dye mixtures, deconvolution techniques were employed to distinguish individual and identify their components maximum absorption wavelengths (λ max). By applying Gaussian fitting, this approach improves the accuracy and reliability of λ max detection and helps to evaluate the selectivity of the adsorbent towards different dyes [44].

The findings indicate that despite the complexity of real wastewater environments, biochar and nano-biochar derived from Areca catechu husks effectively adsorb various dyes, demonstrating their potential as low-cost and sustainable adsorbents. The differences in adsorption percentages highlight the role of surface interactions, electrostatic forces, and functional group availability in influencing dye selectivity. The results also suggest that nano-biochar, due to its superior physicochemical properties, can serve as an efficient adsorbent for wastewater treatment applications involving mixed dye pollutants.

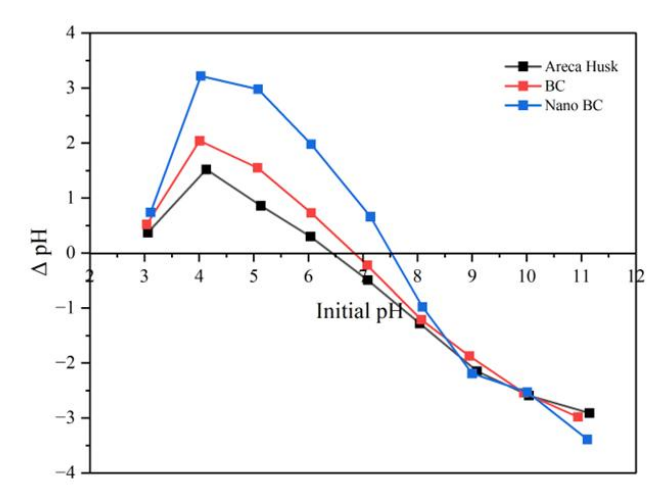


Figure 6. The pH Point Zero Charge (PZC) of areca husk, biochar and nano-biochar

3.3 Impact of pH to Adsorption and pHpzc Determination

This comparative analysis elucidates the progressive morphological changes from raw *Areca* husk to biochar and finally to nano-biochar, underscoring the impact of pyrolysis and particle refinement in tailoring material properties. The graph on Figure 6. illustrates the relationship between the delta pH and the initial pH for biochar and nano-biochar derived from Areca catechu. The pH point of zero charge (pHpzc) for BC and Nano-BC was determined to be approximately 6.94 and 7.53, respectively. The pHpzc is defined as the pH at which the net surface charge of the adsorbent is neutral. Below the pHpzc, the adsorbent's surface is positively charged, thereby facilitating the adsorption of anionic dyes such as Congo red due to electrostatic attraction. Above the pHpzc, the surface acquires a negative charge, thereby reducing the efficiency of adsorption for anionic molecules [38].

The slightly higher pHpzc of Nano-BC in comparison to BC indicates that the nano-biochar exhibits enhanced surface characteristics, which are likely the result of surface modifications achieved through high-energy milling. This modification serves to enhance the surface area and provide a greater number of active sites, thereby improving the performance of the adsorbent at near-neutral pH conditions.

As demonstrated in Figure 7, it is evident that the adsorption capacity of all adsorbents is maximised within the acidic pH range, specifically between pH of 2 and 4, and undergoes a gradual decline as the pH rises. Nano-biochar exhibits the most superior adsorption performance across the entire pH spectrum, with biochar ranking second, while Areca husk demonstrates the least efficient adsorption capacity. This phenomenon is consistent with the pH at the point of zero charge (pHpzc), which determines the net surface charge of an adsorbent. The pHpzc values for BC and

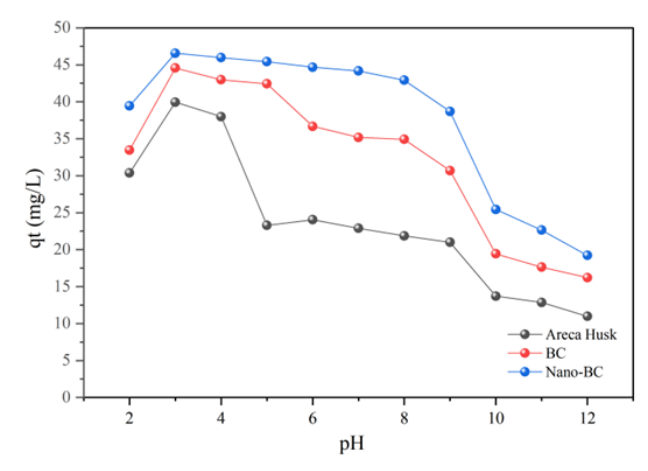


Figure 7. Impact of pH adsorption to arce husk, biochar and nano-biochar

Nano-BC were determined to be approximately 6.94 and 7.53, respectively. This suggests that at lower pH values, the adsorbents' surface is positively charged due to protonation, thereby enhancing the adsorption of anionic dyes like Congo red through electrostatic attraction. Conversely, at higher pH values, the surface charge becomes negative, leading to electrostatic repulsion and a decline in adsorption efficiency.

The superior adsorption capacity exhibited by nano-biochar is attributed to its increased surface area, reduced particle size, and augmented functional groups, which enhance electrostatic interactions and chemical bonding with CR molecules. The adsorption capacity of Nano-BC remains relatively stable from pH of 2 to 6, suggesting strong dye-binding capabilities, before experiencing a sharp decline beyond pH of 8 due to the increasing electrostatic repulsion [46].

These findings on Figure 7 where it shows underscore the pivotal role of pH in adsorption processes and underscore the efficacy of nanobiochar as an advanced adsorbent for dye removal, particularly in acidic environments. The optimized adsorption conditions at lower pH values provide valuable insights for wastewater treatment applications, where pH control can markedly enhance pollutant removal efficiency [47].

3.3 Impact of Adsorption Contact Time

Figure 8 shows the adsorption kinetics of Congo Red by Pinang husk, biochar (BC), and nano-biochar (Nano BC) exhibit notable disparities in performance. The nano-biochar exhibits the highest adsorption capacity, followed by the biochar and the pinang husk, indicating that the nanoscale structure of the nano-biochar provides a larger surface area and more active sites for adsorption [48]. All adsorbents reach equilibrium after approximately 150 minutes, with Nano-BC exhibiting the fastest initial adsorption rate. This indicates that modification of the material through pyrolysis and nanofabrication has a considerable impact on the enhancement of the adsorption performance.

The kinetic data were found to be consistent with both the Pseudo-First-Order (PFO) and Pseudo-Second-Order (PSO) models. However, the Pseudo-Second Order (PSO) model provides a superior fit to the experimental results for all adsorbents, with Nano-BC exhibiting the most pronounced alignment [49]. This suggests that the dominated adsorption process is by chemisorption, which involves chemical interactions, such as hydrogen bonding, π - π interactions, or electrostatic attractions [41]. In contrast, the PFO model provides a less accurate fit, indicating that physical adsorption plays a minor role. The raw Pinang husk shows slower

adsorption kinetics, likely due to its limited porosity and active sites. BC improves adsorption performance by increasing surface area and functional groups, while Nano-BC outperforms both due to its nanoscale features [3]. These findings suggest that Nano-BC is a promising material for dye removal in wastewater treatment. However, its synthesis cost and complexity should be carefully considered.

The adsorption kinetics of Congo Red onto Pinang husk, biochar (BC), and nano-biochar (Nano-BC) can be discussed in light of the graphical representation and Table 1. The experimental adsorption capacities (Qe_{exp}) demonstrate that Nano-BC attains the highest value (46.499 mg/g), followed by BC (44.432 mg/g) and Pinang husk (35.495 mg/g). This suggests that the enhanced surface area and active sites of Nano-BC, resulting from nanoscale its modification, are instrumental in enhancing the efficiency of the adsorption process.

The suitability of the adsorption data for the Pseudo-First-Order (PFO) and Pseudo-Second-Order (PSO) models provides further evidence of the underlying adsorption mechanisms. The R² values for the PSO model are consistently higher (0.999) across all adsorbents compared to the PFO model (R² ranging from 0.722 to 0.866). This evidence indicates that the adsorption process is dominated by chemisorption, which involves interactions such as hydrogen bonding and electrostatic forces between the adsorbate (Congo Red) and the adsorbent surface [42]. Furthermore, the calculated values of Qe from the PSO model are more closely aligned with the experimental values than those from the PFO model, providing additional support \mathbf{for} $_{
m the}$ chemisorption mechanism.

The kinetic rate constants (k_2) from the PSO model provide further insights. The nano-BC exhibits a slightly elevated value for the kinetic

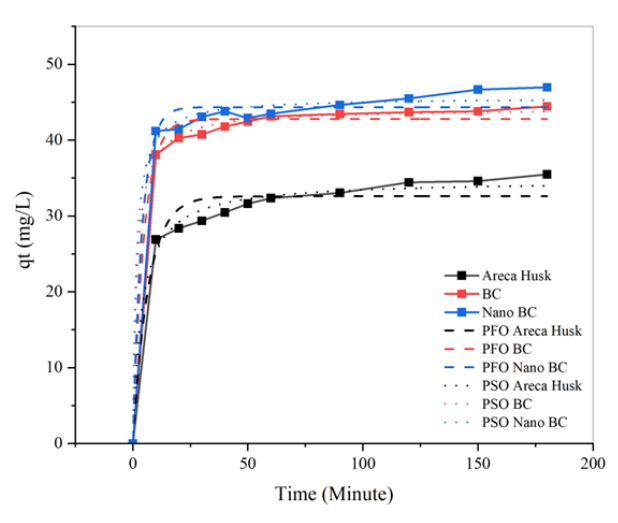


Figure 8. The impact of adsorption contact time by areca husk, biochar and nano-biochar

rate constant at 0.005, in comparison to that of Pinang husk, which is 0.004. This reflects a more rapid adsorption rate, attributable to enhanced surface reactivity [43]. Similarly, BC exhibits the highest value of the kinetic rate constant, k_2 (0.008), which is likely attributable to its balanced porosity and surface functionality.

The graph serves to corroborate these findings, visually illustrating the faster adsorption rate and higher equilibrium capacity of Nano-BC. The kinetics of pinang husk are slower, resulting in a lower adsorption capacity due to the limited surface area and the number of active sites. While BC outperforms Pinang husk, it is slightly less effective than Nano-BC, which exhibits rapid initial adsorption followed by equilibrium at the highest capacity.

Nano-BC has been identified as the most effective adsorbent for Congo Red, demonstrating both high adsorption capacity and rapid kinetics. The PSO model has been shown to accurately describe the adsorption process, indicating that chemisorption is the dominant mechanism [44]. These results emphasise the benefits of material modification and highlight the potential of Nano-BC for practical applications in dye removal from wastewater.

3.4 Impact of Concentration and Temperature on Adsorption

Figure 9 illustrates the effect of initial Congo Red concentration and adsorption temperature on

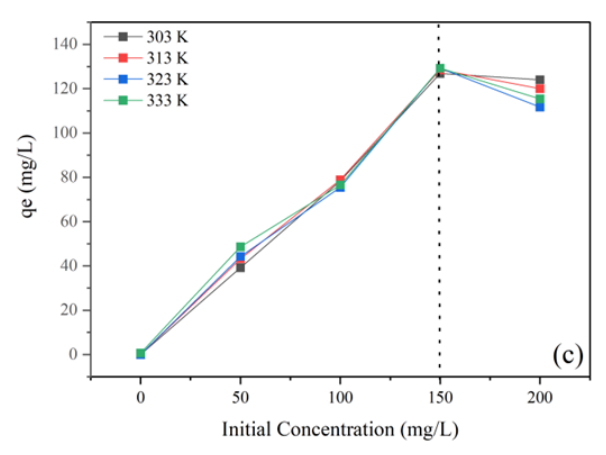


Figure 9. Effect of Initial Concentration congo red and adsorption temprature on Areca husk (a), Biochar (b) and Nano-biochar (c)

Areca husk (a), Biochar (b), and Nano-biochar (c). The adsorption capacity (q_e) increases with initial dye concentration until equilibrium is reached, beyond which no significant enhancement in adsorption is observed. For *Areca* husk (a), equilibrium is reached at approximately 150 mg/L, with adsorption capacity stabilizing at higher temperatures (323 K and 333 K). Biochar (b) exhibits improved adsorption performance, with equilibrium occurring between 150–175 mg/L, and maximum adsorption observed at 333 K. Meanwhile, Nano-biochar (c) demonstrates the most efficient adsorption, achieving equilibrium at 150 mg/L across all temperatures, indicating a rapid and effective adsorption process.

The trend suggests increasing temperature enhances adsorption efficiency, likely due to the endothermic nature of the Additionally, significant process. the improvement in adsorption capacity from Areca husk to Nano-biochar highlights the role of particle size reduction in increasing surface area and active sites, making nano-biochar the most effective adsorbent. The adsorption characteristics of Congo red on Areca husk, BC, and nano-BC were analysed using the Langmuir and Freundlich isotherm models were shown in Table 2. The Langmuir isotherm postulates that adsorption occurs on a uniform surface with monolayer coverage [45]. The key parameters are Qmax, which represents the maximum adsorption capacity, and $k_{\rm L}$, which is the affinity constant. The Freundlich isotherm, an empirical model, is used to describe adsorption on heterogeneous surfaces with varying adsorption energies [46]. It is characterised by two key parameters: $k_{\rm F}$, which represents the relative adsorption capacity, and n, which describes the adsorption intensity.

The Langmuir model indicates that the maximum adsorption capacity ($Q_{\rm max}$) of Congo red on Areca husk is 379.679 mg/g at 60 °C, thereby demonstrating that higher temperatures enhance the adsorption process. Nevertheless, the R² values (0.180–0.784) indicate a poor fit to the Langmuir model, while the low $k_{\rm L}$ values (0.002–0.011) reflect a limited affinity between the adsorbate and the adsorbent [47]. In contrast, the Freundlich model demonstrates a superior alignment with R² values reaching 0.910 at 50 °C. The $k_{\rm F}$ values reach a maximum at 4.529 at 50 °C,

Table 1. The kinetic parameters PFO and PSO models by areca husk, biochar and nano-biochar.

Adsorbent	$Q{ m e}_{ m exp} \ ({ m mg/g})$		PFO			PSO		
		$Q m e_{ m calc} \ (mg/g)$	R^2	k_1	$Q\mathrm{e_{\mathrm{calc}}}\ (\mathrm{mg/g})$	R^2	k_2	
Areca husk	35.495	13.428	0.866	-8.412	36.31	0.999	0.004	
BC	44.432	8.996	0.722	-9.073	44.769	0.999	0.008	
Nano BC	46.499	12.704	0.775	-9.533	47.48	0.999	0.005	

indicating a favourable adsorption capacity, while the n values (1.255–1.578) suggest moderately strong adsorption. With regard to BC, the Langmuir model indicates the highest Q_{max} of 594.406 mg/g at 30 °C, although this decreases with increasing temperature. While the R² values exhibit considerable variation (0.014–0.903), the $k_{\rm L}$ values demonstrate an increase at elevated temperatures. indicative ofan adsorbate-adsorbent interaction. The Freundlich model provides a superior fit at 50 °C, with an R² value of 0.497 and the highest k_F value of 21.192, indicating a considerable relative adsorption capacity. Furthermore, the n values (1.483–2.426) indicate favourable adsorption under these conditions [48].

Nano-BC displays superior adsorption characteristics. The Langmuir model demonstrates consistent Q_{max} across temperatures, with the highest value observed at 154.526 mg/g at 40 °C. It is noteworthy that the R² values for the Langmuir model (0.924–0.980) indicate excellent agreement, while the $k_{\rm L}$ values (0.063-0.115) reflect a high affinity [49]. Furthermore, the Freundlich model demonstrates an excellent fit, with R2 values exceeding 0.926 at all temperatures. Nano-BC attains the highest $k_{\rm F}$ value of 47.259 at 50 °C, thereby exhibiting the most elevated relative adsorption capacity. Moreover, the n values (2.756-4.216) indicate favourable adsorption, thereby emphasising the efficiency of Nano-BC. In conclusion, the Freundlich model provides a superior description of the adsorption process for these adsorbents, particularly for BC and Nano-BC, due to the heterogeneous nature of their surfaces. Among the adsorbents, Nano-BC is the most effective, offering high adsorption capacities, strong adsorbate-adsorbent affinity, and excellent alignment with both isotherm models.

A comparison of adsorption capacities indicates that Nano-BC derived from *Areca* catechu exhibits higher adsorption performance than biochar from other sources, such as pine sawdust, cornstalk, and green pea peels. The higher adsorption capacity of Nano-BC is attributed to the increased specific surface area and greater number of active sites, achieved through particle size reduction via high-energy milling. Thus, nano-biochar has significant potential as a superior adsorbent for wastewater treatment applications.

Table 3 display thermodynamic parameters of adsorption for each adsorbent, including Areca husk, BC, and nano-BC, are presented in tabular form. The thermodynamic analysis demonstrates that the adsorption process exhibits notable variation among the three materials, as evidenced by alterations in enthalpy (Δ H), entropy (Δ S), and Gibbs free energy (Δ G) at varying temperatures [56]. The Δ H value of 13.246 kJ/mol for Areca husk indicates that the adsorption process is endothermic. The positive value of Δ S, which is 0.041 J/mol K, indicates an increase in randomness at the solid-liquid interface during the adsorption process [57]. However, the Gibbs

Table 2. The adsorption isotherm Langmuir and Freundlich parameters by areca husk, biochar and nanobiochar.

Adsorbent	Adsorption	Adsorption	Temperature (T)					
	Isotherm	Constant	30 ℃	40 °C	50 °C	60 °C		
<i>Areca</i> husk	Langmuir	\mathbf{Q}_{max}	123.784	177.509	163.570	379.679		
		$k_{ m L}$	0.083	0.007	0.011	0.002		
		\mathbb{R}^2	0.998	0.383	0.784	0.180		
	Freundlich	$k_{ m F}$	24.272	2.948	4.529	1.111		
		\mathbb{R}^2	0.916	0.695	0.910	1.089		
		n	2.831	1.408	1.578	0.861		
BC	Langmuir	\mathbf{Q}_{max}	117.767	192.200	167.225	308.297		
		$k_{ m L}$	0.031	0.018	0.038	0.009		
		\mathbb{R}^2	0.924	0.878	0.903	0.457		
	Freundlich	$k_{ m F}$	4.725	7.832	21.192	5.059		
		\mathbb{R}^2	0.286	0.863	0.497	0.743		
		n	1.483	1.616	2.426	1.309		
Nano-BC	Langmuir	\mathbf{Q}_{max}	174.200	150.328	149.692	154.526		
		$k_{ m L}$	0.099	0.063	0.115	0.066		
		\mathbb{R}^2	0.903	0.956	0.924	0.952		
	Freundlich	$k_{ m F}$	28.085	25.423	47.259	26.872		
		\mathbb{R}^2	0.956	0.933	0.926	0.935		
		n	3.350	2.730	4.216	2.756		

free energy (ΔG) values exhibit a temperature-dependent variation, shifting from a positive value at 303 K (0.901 kJ/mol) to a negative value at 333 K (-0.321 kJ/mol). This suggests that the adsorption process becomes spontaneous at higher temperatures.

In the case of BC, the ΔH value is 14.729 kJ/mol, indicating a more endothermic process than that observed for Areca husk. The ΔS value of 0.054 J/mol K indicates a moderate increase in entropy during the adsorption process. The Gibbs free energy (ΔG) values are consistently negative across all temperatures, starting from -1.744 kJ/mol at 303 K to -3.375 kJ/mol at 333 K. This consistent negativity indicates that the adsorption process is spontaneous and becomes more favourable with increasing temperature [58].

The highest ΔH value of 23.567 kJ/mol is exhibited by Nano-BC, indicating a markedly endothermic process. The ΔS value of 0.095 J/mol K indicates the greatest increase in entropy among the three adsorbents, which is likely due to the highly active surface and enhanced interaction sites of Nano-BC [59]. The ΔG values for Nano-BC are the most negative, ranging from -5.193 kJ/mol at 303 K to -8.040 kJ/mol at 333 K. This demonstrates that Nano-BC not only exhibits the highest spontaneity but also the most favourable adsorption process at all tested temperatures.

In conclusion, the thermodynamic parameters indicate that the adsorption process

for all adsorbents is endothermic and becomes more spontaneous with increasing temperature. Of the three adsorbents, Nano-BC displays the most effective and spontaneous adsorption behaviour, making it the most efficient material for the removal of Congo red dye.

Table 4 shows a comparison of adsorption capacities indicates that Nano-BC derived from catechu exhibits higher adsorption performance than biochar from other sources, such as pine sawdust [19], cornstalk [69], and green pea peels [66]. The higher adsorption capacity of Nano-BC is attributed to the increased specific surface area and greater number of active sites, achieved through particle size reduction via high-energy milling [41]. Thus, Nano-BC has significant potential as a superior adsorbent for wastewater treatment applications. significant potential as a superior adsorbent for wastewater treatment applications.

Figure 10 shows the spectrum of FTIR analysis before and after adsorption revealed significant changes in the functional groups of Nano-BC and BC. After adsorption, the intensity of the absorption band at 1595 cm⁻¹ (C=C aromatic) shifted and decreased, indicating interactions between Congo Red and the aromatic structure of the adsorbent [70]. Additionally, shifts in the carbonyl (C=O) band around 1710 cm⁻¹ and the hydroxyl (O-H) band at 3200–3500 cm⁻¹ suggest the involvement of hydrogen bonding in the adsorption mechanism [71]. These spectral changes support an adsorption mechanism

Table 3. The adsorption thermodynamic parameter by areca husk, biochar and nano-biochar

Adsorbent	ΔΗ	ΔS	ΔG (kJ/mol)				
	(kJ/mol)	(J/mol K)	303 °K	313 °K	323 °K	333 °K	
Areca husk	13.246	0.041	0.901	0.494	0.086	-0.321	
BC	14.729	0.054	-1.744	-2.288	-2.831	-3.375	
Nano BC	23.567	0.095	-5.193	-6.142	-7.09	-8.040	

Table 4. The comparison of Q_{max} of some biochar from seferal dye sorption related to this work

Adsorbent	Adsorbate	$Q_{ m max}~({ m mg/g})$	Reference
Pine wood	Methylene blue	3.99	[50]
Cornstalk	Procion red	15.9	[28]
Paper and pulp sludge	Methyl orange	20.53	[51]
Straw	Sunset yellow	17.9	[52]
Green pea peels	Congo red	62.11	[53]
Betel nut husk	Congo red	40.616	[54]
Pine neddle	Congo red	30.76	[6]
Pecan Shells	Congo red	130.48	[55]
Zinc oxide green pea peels biochar	Congo red	114.94	[53]
nanocomposite			
Nano-biochar Areca Husk	Congo red	154.526	This study

involving electrostatic interactions, hydrogen bonding, and π - π interactions between the aromatic structure of biochar and the Congo Red molecules [72]. Therefore, the observed FTIR spectral modifications confirm that adsorption occurs not only through physical interactions but also through chemical processes that enhance dye retention within the adsorbent structure [73].

3.5 Regeneration of Adsorbent

regeneration of adsorbents is of paramount importance for the maintenance of the efficiency and reusability of materials employed in adsorption processes. The data pertaining to the adsorption process over four cycles evinces a decline in the efficiency of adsorption for all materials as the number of cycles increases [60]. This decline is visually represented in Figure 11. In the initial cycle (Cycle 0), Nano-BC exhibited the highest adsorption efficiency at 95.04%. followed by BC at 78.82% and Areca husk at 60.32%. This result serves to highlight the enhanced adsorption capability of Nano-BC, which is likely due to its higher surface area and optimised pore size.

As the regeneration cycles progressed, a decline in the adsorption performance of all adsorbents was observed. Following the initial cycle, Nano-BC exhibited a pronounced decline in adsorption efficiency, reaching 38.42% in Cycle 1, and subsequently declining to 26.40% in Cycle 2 and 16.30% in Cycle 3. This rapid decline may be indicative of structural degradation or the loss of active sites due to repeated use. In contrast, BC demonstrated superior retention of its adsorption performance over the course of the cycles, with a decrease from 78.82% in Cycle 0 to 45.21% in Cycle 3 [61]. The lowest overall adsorption efficiency and the steepest decline were observed

for *Areca* husk, which dropped from 60.32% in Cycle 0 to 20.27% in Cycle 3.

The data indicates that whilst Nano-BC exhibits the highest initial adsorption capacity, its regeneration efficiency significantly diminishes after the first cycle. In contrast, BC demonstrates a more consistent performance across cycles, making it a more durable adsorbent for repeated use. Although *Areca* husk is less effective overall, it may still be a cost-effective option for single-use applications.

4. Conclusion

The synthesis and characterization of Areca catechu husk-derived biochar (BC) and nanobiochar (Nano-BC) have been successfully conducted. demonstrating significant improvements in adsorption performance. The structural transformation from raw biomass to Nano-BC was confirmed through XRD, FTIR, and analyses. which revealed enhanced

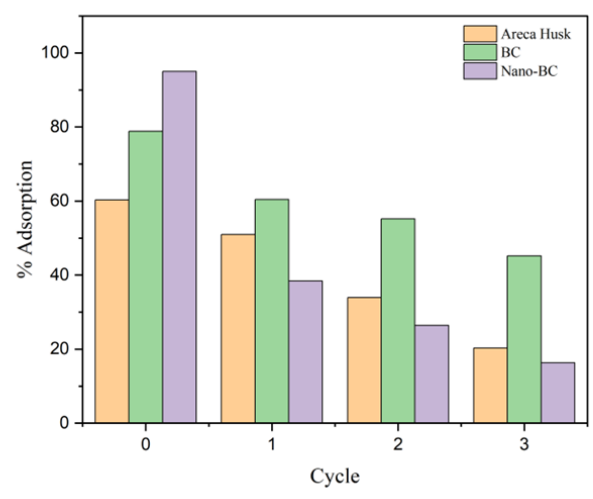


Figure 11. Regeneration cycle of adsorption areca husk, biochar and nano-biochar.

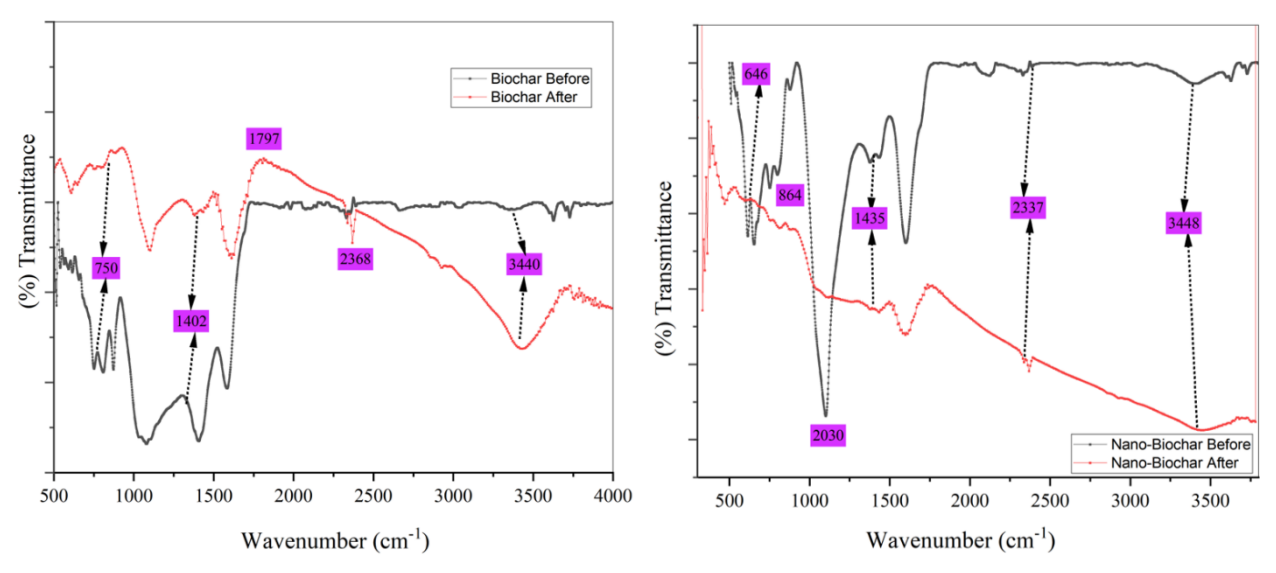


Figure 10. FTIR spectrum of biochar and nano-biochar before and after adsorption

crystallinity, the presence of functional groups conducive to adsorption, and a substantial increase in surface area and porosity. The adsorption kinetics followed a Pseudo-Second-Order (PSO) model, indicating a chemisorptiondominated process, while isotherm studies confirmed favorable adsorption behavior, with Nano-BC exhibiting the highest adsorption capacity. Thermodynamic analyses validated the spontaneity and feasibility of the adsorption process. The findings highlight the novelty of this study in successfully synthesizing a nanomaterial from biomass, offering an efficient and sustainable approach to dye removal. However, while Nano-BC possesses a high adsorption capacity, its small particle size poses challenges in separation post-adsorption, making practical applications more complex. To address this limitation, composite materials or additional structural modifications may be required to facilitate easier recovery in real wastewater treatment scenarios. Future research should investigate the adsorption performance of Nano-BC with other selective dyes and explore strategies to enhance its reusability and scalability for industrial applications.

Acknowledgements

The authors would like to express their gratitude to the Research Centre for Inorganic Materials and Complexes, FMIPAUniversitas Sriwijaya, for their invaluable assistance in providing laboratory analysis. This research also the additional output from SATEKS Unsri grant, number 0012/UN9/SK.LP2M.PT/2024. Furthermore, the authors would like to express their gratitude to the National Research and Innovation Agency (BRIN) for their assistance in pyrolysis process the and material characterisation.

CRediT Author Statement Author

Author contribution Robiatul Adawiyah: Formal analysis, Roles/Writing - original draft, Investigation; Nova Yuliasari: Supervision, Validation, Writing - review & editing; Yulizah Hanifah: Methodology; Project administration, Resources, Software; Neza Rahayu Palapa: Conceptualization, Data curation, Funding acquisition, Visualization, Writing - review & editing. All authors have read and agreed to the published version of the manuscript.

References

- [1] Gamboa, D.M.P., Abatal, M., Lima, E., Franseschi, F.A., Ucán, C.A., Tariq, R., Elías, M.A.R., Vargas, J. (2024). Sorption Behavior of Azo Dye Congo Red onto Activated Biochar from Haematoxylum campechianum Waste: Gradient Boosting Machine Learning-Assisted Bayesian Optimization for Improved Adsorption Process. International Journal of Molecular Sciences, 25(9), 4771. DOI: 10.3390/ijms25094771.
- [2] Lu, X., Jordan, B., Berge, N.D. (2012). Thermal conversion of municipal solid waste via hydrothermal carbonization: Comparison of carbonization products to products from current waste management techniques. Waste Management, 32(7), 1353–1365. DOI: 10.1016/j.wasman.2012.02.012.
- [3] Khan, A.A., Naqvi, S.R., Ali, I., Farooq, W., Anjum, M.W., AlMohamadi, H., Lam, S.S., Verma, M., Ng, H.S., Liew, R.K. (2023). Algal biochar: A natural solution for the removal of Congo red dye from textile wastewater. *Journal of the Taiwan Institute of Chemical Engineers*, 105312. DOI: 10.1016/j.jtice.2023.105312.
- [4] Waly, S.M., El-Wakil, A.M., Abou El-Maaty, W.M., Awad, F.S. (2024). Hydrothermal synthesis of Mg/Al-layered double hydroxide modified water hyacinth hydrochar for remediation of wastewater containing mordant brown dye. RSC Advances, 14(22), 15281–15292. DOI: 10.1039/D4RA02624A.
- [5] Naseem, K., Farooqi, Z.H., Begum, R., Irfan, A. (2018). Removal of Congo red dye from aqueous medium by its catalytic reduction using sodium borohydride in the presence of various inorganic nano-catalysts: A review. *Journal of Cleaner Production*, 187, 296–307. DOI: 10.1016/j.jclepro.2018.03.209.
- [6] Wang, Z., Tang, Z., Xie, X., Xi, M., Zhao, J. (2022). Salt template synthesis of hierarchical porous carbon adsorbents for Congo red removal. Colloids and Surfaces A: Physicochemical and Engineering Aspects, 648, 129278. DOI: 10.1016/j.colsurfa.2022.129278.
- [7] Harja, M., Buema, G., Bucur, D. (2022). Recent advances in removal of Congo Red dye by adsorption using an industrial waste. *Scientific Reports*, 12(1), 6087. DOI: 10.1038/s41598-022-10093-3.
- [8] Hua, Z., Pan, Y., Hong, Q. (2023). Adsorption of Congo red dye in water by orange peel biochar modified with CTAB. RSC Advances, 13(18), 12502–12508. DOI: 10.1039/D3RA01444D.
- [9] Pi, Y., Duan, C., Zhou, Y., Sun, S., Yin, Z., Zhang, H., Liu, C., Zhao, Y. (2022). The effective removal of Congo Red using a bio-nanocluster: Fe3O4 nanoclusters modified bacteria. *Journal of Hazardous Materials*, 424, 127577. DOI: 10.1016/j.jhazmat.2021.127577.
- [10] Li, Y., Meas, A., Shan, S., Yang, R., Gai, X. (2016). Production and optimization of bamboo hydrochars for adsorption of Congo red and 2-naphthol. *Bioresource Technology*, 207, 379–386. DOI: 10.1016/j.biortech.2016.02.012.

- [11] Swan, N.B., Zaini, M.A.A. (2019). Adsorption of Malachite Green and Congo Red Dyes from Water: Recent Progress and Future Outlook. *Ecological Chemistry and Engineering S*, 26(1), 119–132. DOI: 10.1515/eces-2019-0009.
- [12] Swan, N.B., Zaini, M.A.A. (2019). Adsorption of Malachite Green and Congo Red Dyes from Water: Recent Progress and Future Outlook. *Ecological Chemistry and Engineering S*, 26(1), 119–132. DOI: 10.1515/eces-2019-0009.
- [13] Siregar, P.M.S.B.N., Palapa, N.R., Wijaya, A., Fitri, E.S., Lesbani, A. (2021). Structural Stability of Ni/Al Layered Double Hydroxide Supported on Graphite and Biochar Toward Adorption of Congo Red. Science and Technology Indonesia, 6 (2), 85–95. DOI: 10.26554/sti.2021.6.2.85-95.
- [14] Mahmoud, A.E.D., Ali, R., Fawzy, M. (2024). Insights into levofloxacin adsorption with machine learning models using nano-composite hydrochars. *Chemosphere*, 355, 141746. DOI: 10.1016/j.chemosphere.2024.141746.
- $[15] \quad \text{Chao, F.-L., Yang, T.-H., Wu, J.-Y. (2020). New} \\ \text{uses for Areca Catechu tree. } International \ Wood \\ Products \quad Journal, \quad 11(2), \quad 94-100. \quad \text{DOI:} \\ 10.1080/20426445.2020.1732525.$
- [16] Bardalai, M., Mahanta, D.K. (2018). Characterisation of Biochar Produced by Pyrolysis from Areca Catechu Dust. *Materials Today: Proceedings*, 5(1), Part 2, 2089-2097. DOI: 10.1016/j.matpr.2017.09.205.
- [17] Peng, W., Liu, Y.-J., Wu, N., Sun, T., He, X.-Y., Gao, Y.-X., Wu, C.-J. (2015). Areca catechu L. (Arecaceae): A review of its traditional uses, botany, phytochemistry, pharmacology and toxicology, *Journal of Ethnopharmacology*, 164, 340-356, DOI: 10.1016/j.jep.2015.02.010.
- [18] Bansal, M., Pal, B. (2025). Synergy of adsorption and visible light-induced photocatalytic degradation of doxycycline by cellulose modified Cu Al layered double hydroxide binary composite. *International Journal of Biological Macromolecules*, 285, 138329. DOI: 10.1016/j.ijbiomac.2024.138329.
- [19] Pandey, D., Daverey, A., Dutta, K., Arunachalam, K. (2022). Enhanced adsorption of Congo red dye onto polyethyleneimineimpregnated biochar derived from pine needles. *Environmental Monitoring and Assessment*, 194(12), 880. DOI: 10.1007/s10661-022-10563-1.
- [20] Laxmi Deepak Bhatlu, M., Athira, P.S., Jayan, N., Barik, D., Dennison, M.S. (2023). Preparation of Breadfruit Leaf Biochar for the Application of Congo Red Dye Removal from Aqueous Solution and Optimization of Factors by RSM-BBD. Adsorption Science & Technology, 2023, DOI: 10.1155/2023/7369027.

- [21] Vinayagam, R., Kandati, S., Murugesan, G., Goveas, L.C., Baliga, A., Pai, S., Varadavenkatesan, T., Kaviyarasu, K., Selvaraj, R. (2023). Bioinspiration synthesis of hydroxyapatite nanoparticles using eggshells as a calcium source: Evaluation of Congo red dye adsorption potential. *Journal of Materials Research and Technology*, 22, 169–180. DOI: 10.1016/j.jmrt.2022.11.093.
- [22] Belay, T., Worku, L.A., Bachheti, R.K., Bachheti, A., Husen, A. (2023). Nanomaterials: introduction, synthesis, characterization, and applications. In: Advances in Smart Nanomaterials and their Applications. Elsevier, pp. 1–21. DOI: 10.1016/B978-0-323-99546-7.00027-6.
- [23] Mathew Tharayil, J., Chinnaiyan, P. (2023). Sustainable waste valorisation: Novel Areca catechu L. husk biochar for anthraquinone dye adsorption Characterization, modelling, kinetics, and isotherm studies. Results in Engineering, 20. DOI: 10.1016/j.rineng.2023.101624.
- [24] Chausali, N., Saxena, J., Prasad, R. (2021). Nanobiochar and biochar based nanocomposites: Advances and applications. *Journal of Agriculture and Food Research*, 5, 100191. DOI: 10.1016/j.jafr.2021.100191.
- [25] Ren, X., Chen, C., Nagatsu, M., Wang, X. (2011). Carbon nanotubes as adsorbents in environmental pollution management: A review. *Chemical Engineering Journal*, 170(2–3), 395– 410. DOI: 10.1016/j.cej.2010.08.045.
- [26] Sudan, S., Kaushal, J., Khajuria, A. (2024). Efficient adsorption of anionic dye (congo red) using copper-carbon dots doped magnetic biochar: kinetic, isothermal, and regeneration studies. Clean Technologies and Environmental Policy, 26(2), 481–497. DOI: 10.1007/s10098-023-02621-0.
- [27] Wibiyan, S., Royani, I., Ahmad, N., Lesbani, A. (2024). Assessing the efficiency, selectivity, and reusability of ZnAl-layered double hydroxide and Eucheuma cottonii composite in removing anionic dyes from wastewater. *Inorganic Chemistry Communications*, 170, 113347. DOI: 10.1016/j.inoche.2024.113347.
- [28] Wijaya, A., Siregar, P.M.S.B.N., Priambodo, A., Palapa, N.R., Taher, T., Lesbani, A. (2021). Innovative Modified of Cu-Al/C (C = Biochar, Graphite) Composites for Removal of Procion Red from Aqueous Solution. Science and Technology Indonesia, 6(4) DOI: 10.26554/sti.2021.6.4.228-234.
- [29] Normah, N., Juleanti, N., Siregar, P.M.S.B.N., Wijaya, A., Palapa, N.R., Taher, T., Lesbani, A. (2021). Size Selectivity of Anionic and Cationic Dyes Using LDH Modified Adsorbent with Low-Cost Rambutan Peel to Hydrochar. Bulletin of Chemical Reaction Engineering & Catalysis, 16(4), 869–880. DOI: 10.9767/bcrec.16.4.12093.869-880.

- [30] Wibiyan, S., Royani, I., Ahmad, N., Lesbani, A. (2024). Assessing the efficiency, selectivity, and reusability of ZnAl-layered double hydroxide and Eucheuma cottonii composite in removing anionic dyes from wastewater. *Inorganic Chemistry Communications*, 170, 113347. DOI: 10.1016/j.inoche.2024.113347.
- [31] Sharma, P.K., Kumar, R., Singh, R.K., Sharma, P., Ghosh, A. (2022). Review on arsenic removal using biochar-based materials. *Groundwater for Sustainable Development*, 17, 100740. DOI: 10.1016/j.gsd.2022.100740.
- [32] Taher, T., Gusti Wibowo, Y., Maulana, S., Rahayu Palapa, N., Rianjanu, A., Lesbani, A. (2023). Facile synthesis of biochar/layered double oxides composite by one-step calcination for enhanced carbon dioxide (CO2) adsorption. *Materials Letters*, 338, 134068. DOI: 10.1016/j.matlet.2023.134068.
- [33] Wijitkosum, S. (2022). Biochar derived from agricultural wastes and wood residues for sustainable agricultural and environmental applications. *International Soil and Water Conservation Research*, 10(2), 335–341. DOI: 10.1016/j.iswcr.2021.09.006.
- [34] Zahara, Z.A., Royani, I., Palapa, N.R., Mohadi, R., Lesbani, A. (2023). Treatment of Methylene Blue Using Ni-Al/Magnetite Biochar Layered Double Hydroxides Composite by Adsorption. Bulletin of Chemical Reaction Engineering & Catalysis, 18(4), 659–674. DOI: 10.9767/bcrec.20049.
- [35] Cabral, L.L., Bottini, R.C.R., Gonçalves, A.J., Junior, M.M., Rizzo-Domingues, R.C.P., Lenzi, M.K., Nagalli, A., Passig, F.H., dos Santos, P.M., de Carvalho, K.Q. (2025). Food dye adsorption in single and ternary systems by the novel passion fruit peel biochar adsorbent. Food Chemistry, 464, 141592. DOI: 10.1016/j.foodchem.2024.141592.
- [36] Qiu, B., Shao, Q., Shi, J., Yang, C., Chu, H. (2022). Application of biochar for the adsorption of organic pollutants from wastewater: Modification strategies, mechanisms and challenges. Sep. Purif. Technol. 300, 121925, DOI: 10.1016/j.seppur.2022.121925.
- [37] Chaukura, N., Murimba, E.C., Gwenzi, W. (2017). Synthesis, characterisation and methyl orange adsorption capacity of ferric oxide–biochar nano-composites derived from pulp and paper sludge. Applied Water Science, 7(5), 2175–2186. DOI: 10.1007/s13201-016-0392-5.
- [38] Wibiyan, S., Royani, I., Ahmad, N., Lesbani, A. (2024). Assessing the efficiency, selectivity, and reusability of ZnAl-layered double hydroxide and Eucheuma cottonii composite in removing anionic dyes from wastewater. *Inorganic Chemistry Communications*, 170, 113347. DOI: 10.1016/j.inoche.2024.113347.
- [39] Abebe, B., Murthy, H.C.A., Amare, E. (2018). Summary on Adsorption and Photocatalysis for Pollutant Remediation: Mini Review. *Journal of Encapsulation and Adsorption Sciences*, 08(04), 225–255. DOI: 10.4236/jeas.2018.84012.

- [40] Wang, D., Liu, L., Jiang, X., Yu, J., Chen, X. (2015). Adsorption and removal of malachite green from aqueous solution using magnetic β-cyclodextrin-graphene oxide nanocomposites as adsorbents. Colloids and Surfaces A: Physicochemical and Engineering Aspects, 466, 166–173. DOI: 10.1016/j.colsurfa.2014.11.021.
- Rojas-Chávez, H., Juárez-García, J.M., Herrera-[41]Rivera, R., Flores-Rojas, E., González-Domínguez, J.L., Cruz-Orea, A., Cayetano-Castro, N., Ávila-García, A., Mondragón-Sánchez, M.L. (2020). The high-energy milling process as a synergistic approach to minimize thermal conductivity ofPbTe nanostructures. Journalof AlloysandCompounds, 820, 153167. DOI: 10.1016/j.jallcom.2019.153167.
- Algethami, J.S., Alhamami, M.A.M., Alqadami, [42] A.A., Melhi, S., Seliem, A.F. (2024). Magnetic grafted-chitosan for enhanced hydrochar efficient adsorption of malachite green dye from aqueous solutions: Modeling, adsorption behavior, and mechanism analysis. International Journalof Biological127767. Macromolecules, 254,DOI: 10.1016/j.ijbiomac.2023.127767.
- [43] Wang, J., Guo, X. (2020). Adsorption isotherm models: Classification, physical meaning, application and solving method. *Chemosphere*, 258, 127279. DOI: 10.1016/j.chemosphere.2020.127279.
- [44] Tabassum, M., Bardhan, M., Novera, T.M., Islam, Md.A., Hadi Jawad, A., Islam, Md.A. (2020). NaOH-Activated Betel Nut Husk Hydrochar for Efficient Adsorption of Methylene Blue Dye. Water, Air, & Soil Pollution, 231(8), 398. DOI: 10.1007/s11270-020-04762-0.
- [45] Kumar, A., Saini, K., Bhaskar, T. (2020). Hydochar and biochar: Production, physicochemical properties and techno-economic analysis. *Bioresour. Technol.* 310, 123442, DOI: 10.1016/j.biortech.2020.123442
- [46] Li, Y., Meas, A., Shan, S., Yang, R., Gai, X., Wang, H., Tsend, N. (2018). Characterization, isotherm and kinetic data for adsorption of Congo red and 2-naphthol on different bamboo hydrochars. *Data in Brief*, 19, 49–54. DOI: 10.1016/j.dib.2018.04.066.
- [47] Wang, D., Liu, L., Jiang, X., Yu, J., Chen, X. (2015). Adsorption and removal of malachite green from aqueous solution using magnetic β-cyclodextrin-graphene oxide nanocomposites as adsorbents. *Colloids and Surfaces A: Physicochemical and Engineering Aspects*, 466, 166–173. DOI: 10.1016/j.colsurfa.2014.11.021.
- [48] Bolbol, H., Fekri, M., Hejazi-Mehrizi, M. (2019). Layered double hydroxide—loaded biochar as a sorbent for the removal of aquatic phosphorus: behavior and mechanism insights. *Arabian Journal of Geosciences*, 12(16), 503. DOI: 10.1007/s12517-019-4694-4.

- [49] Zhang, D.L., Liu, Z.G., Koch, C.C. (2004). Applications of High Energy Mechanical Milling in Processing Advanced Materials: An Overview of the Understanding. *Journal of Metastable and Nanocrystalline Materials*, 20–21, 103–110. DOI: 10.4028/www.scientific.net/JMNM.20-21.103.
- [50] Saba, B., Christy, A.D., Shah, A. (2024). Hydrochar for pollution remediation: Effect of process parameters, adsorption modeling, life cycle techno-economic assessment and evaluation. ConservationandResources. Recycling, 202, 107359. DOI: 10.1016/j.resconrec.2023.107359.
- [51] Bo, J., Shi, B. (2024). Performances of residues from hydrolyzed corn-cobs for the adsorption of Congo red. *Industrial Crops and Products*, 220, 119311. DOI: 10.1016/j.indcrop.2024.119311.
- [52] Haris, M., Khan, M.W., Paz-Ferreiro, J., Mahmood, N., Eshtiaghi, N. (2022). Synthesis of functional hydrochar from olive waste for simultaneous removal of azo and non-azo dyes from water. Chemical Engineering Journal Advances, 9, 100233. DOI: 10.1016/j.ceja.2021.100233.
- [53] Lin, Z., Wang, R., Tan, S., Zhang, K., Yin, Q., Zhao, Z., Gao, P. (2023). Nitrogen-doped hydrochar prepared by biomass and nitrogen-containing wastewater for dye adsorption: Effect of nitrogen source in wastewater on the adsorption performance of hydrochar. Journal of Environmental Management, 334, 117503. DOI: 10.1016/j.jenvman.2023.117503.
- [54] Supraja, K.V., Doddapaneni, T.R.K.C., Ramasamy, P.K., Kaushal, P., Ahammad, Sk.Z., Pollmann, K., Jain, R. (2023). Critical review on production, characterization and applications of microalgal hydrochar: Insights on circular bioeconomy through hydrothermal carbonization. Chemical Engineering Journal, 473, 145059. DOI: 10.1016/j.cej.2023.145059.
- [55] Tu, W., Liu, Y., Xie, Z., Chen, M., Ma, L., Du, G., Zhu, M. (2021). A novel activation-hydrochar via hydrothermal carbonization and KOH activation of sewage sludge and coconut shell for biomass wastes: Preparation, characterization and adsorption properties. *Journal of Colloid and Interface Science*, 593, 390–407. DOI: 10.1016/j.jcis.2021.02.133.
- [56] Singh, D.K., Garg, A. (2024). Application of sewage sludge derived hydrochar as an adsorbent for removal of methylene blue. Sustainable Chemistry for the Environment, 8, 100158. DOI: 10.1016/j.scenv.2024.100158.
- [57] Liu, C., Balasubramanian, P., Li, F., Huang, H. (2024). Machine learning prediction of dye adsorption by hydrochar: Parameter optimization and experimental validation. Journal of Hazardous Materials, 480, 135853. DOI: 10.1016/j.jhazmat.2024.135853.
- [58] Jalilian, M., Bissessur, R., Ahmed, M., Hsiao, A., He, Q.S., Hu, Y. (2024). A review: Hydrochar as potential adsorbents for wastewater treatment and CO2 adsorption. Science of The Total Environment, 914, 169823. DOI: 10.1016/j.scitotenv.2023.169823.

- [59] Mahar, D., Semwal, N., Aneja, A., Arya, M.C. (2024). Rapid adsorptive removal of congo red using Cu/Fe/Al mixed metal oxides obtained from layered double hydroxide nanomaterial: Performance and optimization evaluation using BBD-RSM approach. Surfaces and Interfaces, 55, 105366. DOI: 10.1016/j.surfin.2024.105366.
- [60] Emmanuel, S.S., Adesibikan, A.A. (2024). Hydrothermal valorization of biomass waste into hydrochar towards circular economy and sustainable adsorptive dye contaminants cleanup: A review. *Desalination and Water Treatment*, 320, 100801. DOI: 10.1016/j.dwt.2024.100801.
- [61] Hammud, H.H., Hammoud, M.H., Hussein, A.A., Fawaz, Y.B., Abdul Hamid, M.H.S., Sheikh, N.S. (2023). Removal of Malachite Green Using Hydrochar from PALM Leaves. *Sustainability*, 15(11), 8939. DOI: 10.3390/su15118939.
- [62] Hasanah, M., Wijaya, A., Arsyad, F.S., Mohadi, R., Lesbani, A. (2022). Preparation of Hydrochar from Salacca zalacca Peels by Hydrothermal Carbonization: Study of Adsorption on Congo Red Dyes and Regeneration Ability. Science and Technology Indonesia, 7(3), 372–378. DOI: 10.26554/sti.2022.7.3.372-378.
- [63] Goyi, A.A., Sher Mohammad, N.M., Omer, K.M. (2024). Preparation and characterization of potato peel derived hydrochar and its application for removal of Congo red: a comparative study with potato peel powder. *International Journal of Environmental Science and Technology*, 21(1), 631–642. DOI: 10.1007/s13762-023-04965-y.
- [64] Lonappan, L., Rouissi, T., Das, R.K., Brar, S.K., Ramirez, A.A., Verma, M., Surampalli, R.Y., Valero, J.R. (2016). Adsorption of methylene blue on biochar microparticles derived from different waste materials. Waste Management, 49, 537– 544. DOI: 10.1016/j.wasman.2016.01.015.
- [65] Dai, Y., Zhang, N., Xing, C., Cui, Q., Sun, Q. (2019). The adsorption, regeneration and engineering applications of biochar for removal organic pollutants: A review. *Chemosphere*, 223, 12–27. DOI: 10.1016/j.chemosphere.2019.01.161.
- [66] Rubangakene, N.O., Elwardany, A., Fujii, M., Sekiguchi, H., Elkady, M., Shokry, H. (2023). Biosorption of Congo Red dye from aqueous solutions using pristine biochar and ZnO biochar from green pea peels. *Chemical Engineering Research and Design*, 189, 636–651. DOI: 10.1016/j.cherd.2022.12.003.
- [67] Adawiyah, R., Yuliasari, N., Hanifah, Y., Alawiyah, K., Rahayu Palapa, N. (2024). Utilizing Areca catechu L. Fruit Peel-Derived Biochar and Hydrochar for Congo Red Adsorption: Kinetic and Thermodynamic Analysis. Indonesian Journal of Environmental Management and Sustainability, 8(4), 135–144. DOI: 10.26554/ijems.2024.8.4.135-144.
- [68] Xu, W., Cai, B., Zhang, X., Zhang, Y., Zhang, Y., Peng, H. (2024). The Biochar Derived from Pecan Shells for the Removal of Congo Red: The Effects of Temperature and Heating Rate. *Molecules*, 29(23), 5532. DOI: 10.3390/molecules29235532.

- [69] Guo, S., Dong, X., Wu, T., Shi, F., Zhu, C. (2015). Characteristic evolution of hydrochar from hydrothermal carbonization of corn stalk. *Journal of Analytical and Applied Pyrolysis*, 116, 1–9. DOI: 10.1016/j.jaap.2015.10.015.
- [69] Faheem, Du, J., Bao, J., Hassan, M.A., Irshad, S., Talib, M.A. (2019). Multi-functional Biochar Novel Surface Chemistry for Efficient Capture of Anionic Congo Red Dye: Behavior and Mechanism. Arabian Journal for Science and Engineering, 44(12), 10127–10139. DOI: 10.1007/s13369-019-04194-x.
- [70] Li, H., Budarin, V.L., Clark, J.H., North, M., Wu, X. (2022). Rapid and efficient adsorption of methylene blue dye from aqueous solution by hierarchically porous, activated starbons®: Mechanism and porosity dependence. *Journal of Hazardous Materials*, 436, 129174. DOI: 10.1016/j.jhazmat.2022.129174.
- [71] Peng, W., Liu, Y.-J., Wu, N., Sun, T., He, X.-Y., Gao, Y.-X., Wu, C.-J. (2015). Areca catechu L. (Arecaceae): A review of its traditional uses, botany, phytochemistry, pharmacology and toxicology. *Journal of Ethnopharmacology*, 164, 340–356. DOI: 10.1016/j.jep.2015.02.010.
- [72] Sabio, E., Álvarez-Murillo, A., Román, S., Ledesma, B. (2016). Conversion of tomato-peel waste into solid fuel by hydrothermal carbonization: Influence of the processing variables. *Waste Management*, 47, 122–132. DOI: 10.1016/j.wasman.2015.04.016.